GEOPHYSICAL RESEARCH LETTERS, VOL. 26, NO. 14, PAGES 2219-2222, JULY 15, 1999

Ice particle formation and sedimentation in the tropopause region: A case study based on in situ measurements of total water during POLSTAR 1997

C. Schiller[1], A. Afchine[1], N. Eicke[1], C. Feigl[3], H. Fischer[2], A. Giez[3], P. Konopka[1], H. Schlager[3], F. Tuitjer[1], F. G. Wienhold[2], and M. Zöger[1,3]

Abstract. During the Polar Stratospheric Aerosol Experiment, total water was measured using an airborne Lyman-α fluorescence hygrometer. The inlet is designed for anisokinetic sampling, thus large ice particles are detected sensitively. During the flight on January 24, 1997, temperatures of 200 K occurred close to the tropopause. Within this cold area, the existence of large particles with radii ≥ 4 μm containing large amounts of water is observed. At the edge of this cloud, total water mixing ratios of 5-6 ppmv and close to saturation were measured at and below the tropopause. This observation together with analysis of the correlation of the H_2O mixing ratio with other long-lived tracers indicates that the air masses had been dried by sedimentation of large ice particles.

Introduction

The formation of clouds depends on both the air temperature and the availability of condensable vapors. Stratospheric clouds have been observed only in the very cold regions of the polar vortex over Antarctica and to a lesser extent also in the Arctic. Though temperatures at tropopause altitudes do not reach such low values, higher H_2O mixing ratios, up to 10-20 ppmv in the lowest layers of the stratosphere [e.g. Foot, 1984] may lead to the formation of cirrus clouds. Wang et al. [1996] report subvisual clouds near the tropopause, with highest frequencies at low latitudes where temperatures are lowest.

Most of the studies on stratospheric particle formation made in the past focus on the situation in the lower and middle stratosphere where only slightly variable H_2O mixing ratios around 5 ppmv are expected, and nucleation rates are mainly a function of the abundance of other condensable gases such as HNO_3 and temperature. In the more humid tropopause region, the H_2O mixing ratio becomes - beside temperature - the dominant parameter determining particle formation.

The formation of cirrus clouds in the tropopause region and their impact on trace gas composition is the subject of a number of studies: During the Airborne Arctic Stratospheric Expedition (AASE I) in the Arctic winter, ice saturation was frequently observed close to the tropopause [Murphy et al., 1990]. Jensen et al. [1998] discussed the potential of drying the tropopause region by the formation of cirrus clouds and its dependence on the regional and time scales of cold areas.

Experimental

The Polar Stratospheric Aerosol Experiment (POLSTAR) in January/February 1997 in the Arctic addressed questions of particle formation and its impact on trace gas abundances (e.g. H_2O and HNO_3) in the tropopause region. The instrumentation of the Falcon twin jet aircraft consisted of several in situ experiments to measure O_3, H_2O, NO_y, HNO_3, CO, N_2O, condensation nuclei and particle size distribution. H_2O was measured by the Fast In situ Stratospheric Hygrometer (FISH), based on the Lyman-α photofragment fluorescence technique. A description of the instrument and its calibration is given by *Zöger et al.* [1999]. The time resolution of the hygrometer is 1 s, its precision better than 4%, and the accuracy approximately 0.2 ppmv for stratospheric mixing ratios.

For the inlet, a 1/2" stainless steel tube has been mounted in the forward flight direction at the top of the fuselage at 200 mm distance from the skin, i.e. outside the aircraft's boundary layer and the shadow zone for particle trajectories, assuming their radius r ≤ 20 μm. For flight conditions in the tropopause region, the enhancement of the sampling efficiency for particles with e.g. r = 10 μm due to flow perturbations from the fuselage can be estimated as 11%, using the approximations derived by *King* [1984]. The inlet is connected to the instrument via an electropolished stainless steel tube that is heated to 80°C in order to avoid contamination by adsorption and desorption of water vapor in the inlet line. Thus ice particles entering the inlet are completely evaporated in the instrument. Typical flow rates through the instrument range between 0.3 and 0.7 STP l/s depending on the altitude and speed of the aircraft, corresponding to a residence time of air in the fluorescence cell below 1 s.

The water mixing ratio H_2O_{meas} as measured by FISH includes both the H_2O mixing ratio in the gas phase (H_2O_{gas}) as well as in the condensed phase (H_2O_{cnd}). In ice clouds, H_2O_{gas} is assumed to be in thermodynamic equilibrium with ice, and H_2O_{gas} can be calculated using the empirical equation of *Marti and Mauersberger* [1993]. As long as H_2O_{meas} is less than the saturation mixing ratio, the measurement cannot be occurring in an ice cloud. When H_2O_{meas} exceeds the saturation mixing ratio, the difference must arise from particles entering the inlet.

Due to anisokinetic sampling by the inlet, H_2O_{cnd} is overestimated and corrections for particle sampling efficiency

[1]Institut für Stratosphärische Chemie, Forschungszentrum Jülich GmbH, Jülich, Germany.
[2]Max-Planck-Institut für Chemie, Mainz, Germany.
[3]Deutsches Zentrum für Luft- und Raumfahrt, Weßling, Germany.

Paper number 1999GL900337.
0094-8276/99/1999GL900337$05.00

of the inlet have to be taken into account. The geometry of the inlet causes the aerosol number density N in the probe to differ from the true aerosol number density N_0 in the atmosphere by the so-called enhancement factor $A=N/N_0$. To determine A, we performed fluid dynamical calculations of the flow stream and particle trajectories using a commercial software package (CFX, ASC Ltd., Canada). In Figure 1, A calculated for a compressible fluid is plotted as a function of r and compared to those derived from two other approaches for incompressible fluids [*Belyaev and Levin*, 1974; *Zhang and Liu*, 1989]. The three approaches agree within ±15% for r > 0.5 μm. In passing we note that for smaller particles, the compressible calculations of A do not tend to approach 1 as is expected for incompressible flow. Since cross checks assuming an incompressible flow agree quantitatively with the approach by *Zhang and Liu* [1989], computational errors are not believed to be the reason for the deviations in the enhancement factor for small particles.

Considering a size distribution N(r) of the particles in a cloud, the condensed amount has to be corrected using an effective enhancement factor

$$A_{eff} = \frac{\int A(r) \cdot N(r) \cdot r^3 \cdot dr}{\int N(r) \cdot r^3 \cdot dr} \quad (1)$$

Small particles do not contribute significantly to the overall signal, e.g. a single particle per cm^3 with r = 2 μm results in a signal corresponding to the detection limit of FISH for typical measurement conditions at tropopause altitudes. Based on a size distribution in the range r = 0.15-10 μm, measured using a Multi-angle Aerosol Spectrometer Probe (MASP) [*Feigl et al.*, 1999], particles with r ≥ 4 μm carry more than 95% of the condensed H_2O. Figure 1 shows that for particles with r = 4-10 μm the deviation from an optimized value A_{opt} = 7.9 - which is close to its maximum value - is less than 6%. Thus, the total water mixing ratio $H_2O_{total} = H_2O_{cnd} + H_2O_{gas}$ can be approximated by

$$H_2O_{total} = \left(H_2O_{meas} - H_2O_{gas}\right) / A_{opt} + H_2O_{gas} \quad (2)$$

For measurements in clouds, the uncertainty of H_2O_{total} is determined to be < 25%.

A Lyman-α absorption hygrometer for measurements in the troposphere was operated simultaneously. The inlet

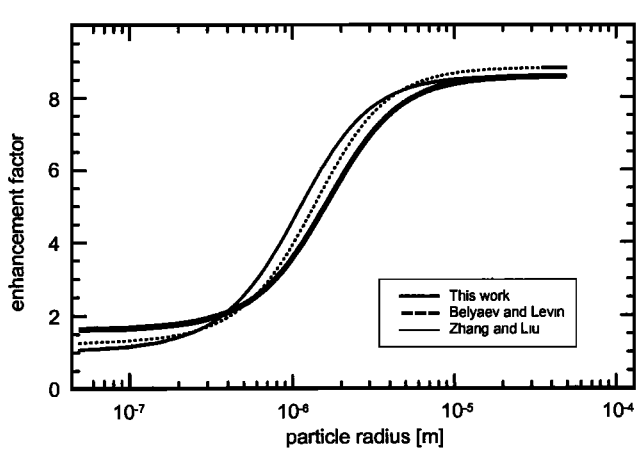

Figure 1: Enhancement factor for the FISH inlet, determined for a compressible fluid using a fluid dynamical software package (this work) in comparison with calculations for the incompressible case.

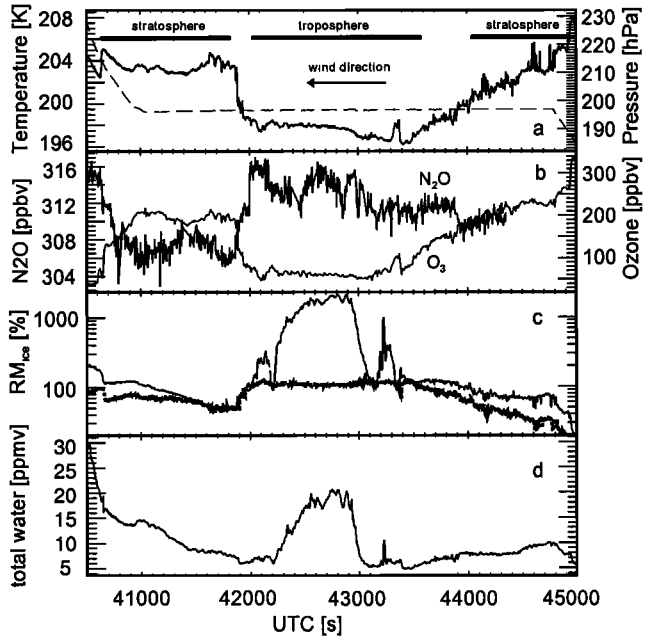

Figure 2: Time series of measurements at the flight level of 200 hPa on January 24, 1997: (a) Temperature (solid line) and pressure (b) N_2O and O_3 (c) Relative mixing ratio RM without correction for anisokinetic sampling artifacts (thin line) and RM measured by the absorption hygrometer for gas phase measurements (d) Total water measured by FISH (corrected).

consists of a total air temperature housing (Rosemount) designed to separate particles from the probed air flow. Quantitative measurements below 20 ppmv cannot be obtained with the absorption hygrometer. However, this instrument is still able to detect relative changes in this range as demonstrated by simultaneous measurements with FISH during flight legs without clouds. When flying in clouds, the data clearly show the qualitative difference in the total water measurements by FISH. The absorption measurements shown below are based on a calibration using the FISH calibration bench. Since the lamp intensity of the absorption hygrometer is not monitored, the remaining systematic differences between the absorption and the FISH measurements may be caused by short-time drifts in lamp intensity.

Results and Discussion

On January 24, 1997, the aircraft crossed a mesoscale region over the Atlantic, northwest of Scandinavia, with a cold tropopause [Figure 1, *Feigl et al.*, 1999]. Trajectory calculations based on ECMWF analyses show that the air masses in this region were lifted up by approximately 100 hPa within the previous 50 hours [*B. Naujokat*, personal communication], thereby adiabatically cooling by more than 20 K. The aircraft probed this area on three flight levels at constant pressures of 200, 180, and 170 hPa. On the two upper flight levels, H_2O mixing ratios of 5-7 ppmv were observed at temperatures between 202 and 207 K, well above the frost point. On the lowest flight level, temperatures below 200 K were measured (Figure 2a). The mixing ratios of other tracers measured simultaneously on board the aircraft are

shown in Figure 2b: N_2O measured by a tunable diode laser spectrometer [*Wienhold et al.*, 1998] and O_3 measured by a photometric detector [*Feigl et al.*, 1999]. The observations of low ozone (≤ 200 ppbv) and high N_2O (≥ 310 ppbv) at 41900-44400 s indicate that the flight track crossed a region of elevated tropopause (Figure 3), in accordance with the trajectory analysis. The measurements along the flight track, which was almost parallel to the horizontal wind vector, represent a sequence of air masses following different trajectories at different altitudes. They can thus be interpreted as a quasi-Lagrangian experiment [*Peter et al.*, 1999].

Here, FISH measurements without the sampling correction ranged from 5 to more than 100 ppmv. The ratio between H_2O_{meas} and the saturation mixing ratio, denoted hereafter as the relative mixing ratio RM, ranged between 0.6 and 20 as plotted in Figure 2c. If RM is significantly larger than 1 (allowing for a certain degree of supersaturation), FISH measurements indicate the existence of particles containing large amounts of water. The gas phase measurements obtained by the absorption hygrometer (thick line in Figure 2c) do not show a corresponding increase of water vapor in the very cold air masses and are close to RM = 1. The existence of particles with r = 1-10 μm has also been identified in the cloud spectrum measured by MASP [*Feigl et al.*, 1999]. Thus the H_2O data need to be corrected for anisokinetic sampling via equation (2) here. After correction, the time series (Figure 2d) still exhibits structure with mixing ratios increasing from less than 10 ppmv (downwind of the coldest area) to approximately 20 ppmv and decreasing again to values below 10 ppmv (upwind of this area), roughly corresponding to the structures in the tracer's abundances and the location of isentropes as they are indicated in Figure 3.

Figure 4 shows again the mixing ratio of total water together with the saturation mixing ratio. The existence of ice particles is evident in air masses with high total water and temperatures below the frost point (42200-43100 s and around 43220 s). On both sides of the ice cloud, measured mixing ratios of total water correspond to the saturation mixing ratio. From significant differences in the measured gas phase and total NO_y mixing ratio [*Feigl et al.*, 1999], growth of smaller particles is also evident, at least on the upwind side of the ice cloud (43100-44400 s). These smaller particles cannot contain a major part of the total water that is detectable by FISH. The MASP particle size spectra, integrated for the ice cloud area and at its edge, are consistent with these observations.

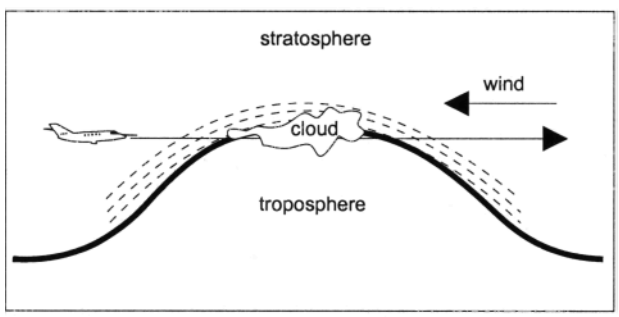

Figure 3: Schematic representation of isentropic trajectories (dashed lines) encountered along the lowest flight track on 970124 at constant pressure.

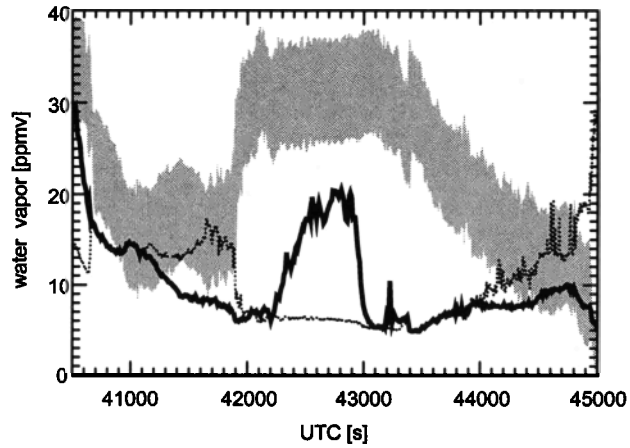

Figure 4: Time series of the flight leg as in Figure 2 of total water (black line), saturation H_2O mixing ratio (dotted line), and the expected climatological range of H_2O (shaded area) calculated from a correlation with O_3.

FISH measurements of water vapor together with those of tracers (N_2O, O_3, and others) across the tropopause performed during the other POLSTAR flights and the Stratosphere-Troposphere Experiments by Aircraft Measurements (May-June 1996 at mid-latitudes, and March 1997 in the Arctic) have been used to derive correlations of the H_2O mixing ratio with those of other tracers [*Eicke*, 1999]. These correlations have been found to vary due to different processes, such as recent intrusions of tropospheric air or local drying. Compared with the other campaigns, the POLSTAR measurements in the Arctic winter yield lowest H_2O abundance around the tropopause, even when the measurements in cold regions close to saturation are not considered. For tropospheric air masses, a lower limit of the expected H_2O mixing ratio can be derived using averaged tropopause values. Using these correlations and the tropospheric minimum as a climatological spread for the high latitude winter, the expected range of H_2O mixing ratios based on the simultaneous measurement of O_3 is included in Figure 4. In the ice cloud itself and the area when the total water mixing ratio corresponds to the saturation mixing ratio (41900-42200 and 43000-44200 s), the measurements are significantly below the climatologically averaged spread, which exhibits already lower H_2O abundances than observed at other locations and seasons.

Similar observations were obtained at the end of the ascent to this flight level (Figures 2 and 4, 40500-40900 s). At 230-220 hPa (40500-40600 s), ice clouds (RM = 2) were observed by FISH, and above the ice cloud (40600-40900 s), H_2O_{total} corresponds to the saturation mixing ratio. Before 40800 s, H_2O_{total} is also below the climatological spread.

H_2O mixing ratios below the climatological spread in air that is saturated, as observed at both edges of the ice cloud, provides strong evidence that the air masses are under the control of the local temperature and have been dried by sedimentation of large ice particles. According to calculations by *Müller and Peter* [1992], sedimentation of particles with r = 10 μm occurs at approximately 100 m/h at 200 hPa and these temperatures. The time for air being exposed to the mesoscale cold area is on the order of a few hours and is therefore sufficient for dehydration of thin layers.

A plausible explanation for the general structure of the cloud is the formation of particles of different size and composition in the cold area. At its edges with air masses from higher θ levels (using the advantage that the experiment is of quasi-Lagrangian type), the large ice particles have already sedimented, and only smaller particles remain. In the core of the cloud, consisting of air masses lifted from the lowest altitudes and thus those with the highest total water abundance, ice particles are still present. Considering the aforementioned time scales, it is likely that these air masses also contain ice particles sedimenting from layers that are higher by a few hundred m. Summarizing this explanation, the observations provide evidence that the cloud would dry from the top.

Summary and Conclusions

At tropopause altitudes outside the tropics, relatively high H_2O mixing ratios of 10-20 ppmv or more lead to particle formation at temperatures even above 200 K and are quite common. In this paper, a high latitude region with an elevated tropopause and adiabatically cooled air masses with temperatures slightly below 200 K was studied. Here, the total water abundance was partially dehydrated to the frost point, that is 5-6 ppmv. These very low mixing ratios observed slightly below the thermal tropopause are of a similar magnitude to those observed in the tropics that determine the entry level of H_2O into the stratosphere there. They are significantly lower than the climatological spread observed at these levels outside such cold events. Such limited local events may dry the tropopause region on larger regional scales persistently and may thus be responsible for its observed dryness in the Arctic winter [*Murphy et al.*, 1990; *Eicke*, 1999].

Feigl et al. [1999] and *Meilinger et al.* [1999] argue that a major part of NO_y in this air mass has remained in the gas phase or might have been present as smaller ternary solution droplets. The studies suggest that only little HNO_3 was taken up by the larger ice particles. *Meilinger et al.* explain that adiabatic cooling of the air and its chemical composition led to the formation of a large size spectrum of particles, allowing the coexistence of large ice particles and smaller liquid droplets. However, considering the full range of uncertainties of the HNO_3 measurements, the observations might also imply that the fraction of HNO_3 to NO_y was below 10%, and thus even lower than in the findings of *Weinheimer et al.* [1998], indicating that the air masses have been denitrified in a previous event probably caused by subsidence of ice particles and subsequent dehydration.

The measurements show that in such cold mesoscale regions, formation and subsequent sedimentation of ice clouds dries the air on time scales of a few hours, but does not necessarily remove NO_y simultaneously to a larger extent. One could imagine that similar processes could also occur at higher stratospheric levels in mountain wave induced ice clouds, though the composition of condensable gases is different there.

Acknowledgements. The measurements have been supported by BMBF under contract 01LO9313. Logistical support and aircraft operation of the DLR flight department are gratefully acknowledged as well as the meteorological forecasts and analysis by B. Naujokat, A. Doernbrack, and H. Volkert and discussions with S. Meilinger, T. Peter, O. Bujok, and D. S. McKenna. Thanks for excellent comments on the manuscript by E. Hintsa.

References

Belyaev, S. P. and L. M. Levin, Techniques for collection of representative aerosol samples, *J. Aerosol Sci., 5*, 325-338, 1974.

Eicke, N., In-situ Messung von Wasserdampf in der unteren Stratosphäre und im Bereich der Tropopause (in German), PhD thesis, Rhein. Friedrich Wilhelms Univ. Bonn, 1999.

Feigl, C., et al., Observation of NO_y uptake by ice particles in the Arctic tropopause region at low temperatures, *Geophys. Res. Lett.*, in press, 1999.

Foot, J. S., Aircraft measurements of the humidity in the lower stratosphere from 1977 to 1980 between 45°N and 65°N, *Q. J. R. Meteorol. Soc., 110*, 303-319, 1984.

Jensen, E. J., et al., Ice nucleation processes in upper tropospheric wave-clouds observed during SUCCESS, *Geophys. Res. Lett., 25*, 1363-1366, 1998.

King, W. D., Air flow and particle trajectories around aircraft fuselages. I: Theory, *J. Atmos. Oceanic Tech., 1*, 5-13, 1984.

Marti, J. and K. Mauersberger, A survey and new measurements of ice vapor pressure at temperatures between 170 and 250 K, *Geophys. Res. Lett., 20*, 363-366, 1993.

Meilinger, S., et al., HNO_3 partitioning in cirrus clouds, *Geophys. Res. Lett.*, in press, 1999.

Müller, R. and Th. Peter, The numerical modelling of the sedimentation of polar stratospheric cloud particles, *Ber. Bunsenges. Phys. Chem., 96*, 353-361, 1992.

Murphy, D. M. et al., Ice saturation at the tropopause observed from the ER-2 aircraft, *Geophys. Res. Lett., 17*, 353-356, 1990.

Peter, T., S. K. Meilinger, and K. S. Carslaw, Quasi-Lagrangian measurements of clouds at and above the tropopause, *SPARC Newsletter, 12*, 14-17, 1999.

Wang, P.-H., P. Minnis, M. P. McCormick, G. S. Kent, and K. M. Skeens, A 6-year climatology of cloud occurence frequency from Stratospheric Aerosol and Gas Experiment II observations (1985-1990), *J. Geophys. Res., 101*, 29,407-29,429, 1996.

Weinheimer, A. J., et al., Uptake of NO_y on wave-cloud ice particles, *Geophys. Res. Lett., 25*, 1725-1728, 1998.

Wienhold, F. et al., TRISTAR - a tracer in situ TDLAS for atmospheric research, *Appl. Phys. B, 67*, 411-417, 1998.

Zhang, Z. Q. and B. Y. H. Liu, On the empirical fitting equations for aspiration coefficients for thin-walled sampling probes, *J. Aerosol Sci., 20*, 713-720, 1989.

Zöger, M. et al., Fast in situ hygrometers: A new family of ballonborne and airborne Lyman-α photofragment fluorescence hygrometers, *J. Geophys. Res., 104*, 1807-1816, 1999.

A. Afchine, N. Eicke, P. Konopka, C. Schiller, and F. Tuitjer, Institut für Stratosphärische Chemie, Forschungszentrum Jülich, 52425 Jülich, Germany. (e-mail: c.schiller@fz-juelich.de)

C. Feigl, A. Giez, H. Schlager, and M. Zöger, Deutsches Zentrum für Luft- und Raumfahrt, Weßling, Germany.

H. Fischer and F. G. Wienhold, Max-Planck-Institut für Chemie, Mainz, Germany.

(Received: December 29, 1998; revised: March 1, 1999; accepted: March 30, 1999)